2016

Retinoid Regulation of Antiviral Innate Immunity in Hepatocytes

Noell E. Cho
University of Southern California

Bo-Ram Bang
University of Southern California

Purnima Gurung
University of Southern California

Meng Li
University of Southern California

Dahn L. Clemens
University of Nebraska Medical Center, dclemens@UNMC.edu

See next page for additional authors

HEPATOLOGY

HEPATOLOGY, VOL. 63, NO. 6, 2016

Retinoid Regulation of Antiviral Innate Immunity in Hepatocytes

Noell E. Cho,[1] Bo-Ram Bang,[1] Purnima Gurung,[1] Meng Li,[3] Dahn L. Clemens,[4] T. Michael Underhill,[5] Laura P. James,[6] Jenifer R. Chase,[7] and Takeshi Saito[1,2]

Persistent infection of hepatitis C virus (HCV) is one of the leading causes of end-stage liver disease (ESLD), such as decompensated cirrhosis and liver cancer. Of particular note, nearly half of HCV-infected people in the United States are reported to be heavy drinkers. This particular group of patients is known to rapidly progress to the ESLD. Although accelerated disease progression among alcohol abusers infected with HCV is clinically well recognized, the molecular pathophysiology behind this manifestation has not been well elucidated. Hepatocytes metabolize ethanol (EtOH) primarily through two steps of oxidative catabolism in which alcohol dehydrogenase (ADH) and aldehyde dehydrogenase (ALDH) play central roles. The ADH-ALDH pathway also governs the metabolism of retinol (vitamin A) to its transcriptionally active metabolite, retinoic acid (RA). In this study, we defined that the ADH-ALDH pathway serves as a potent antiviral host factor in hepatocytes, which regulates the expression of interferon (IFN)-stimulated genes (ISGs) by biogenesis of RA. ISGs constitute over 300 antiviral effectors, which cooperatively govern intracellular antiviral innate immunity. Our study revealed that intracellular RA levels greatly influence ISG expression under basal conditions. Moreover, RA augments ISG induction in response to viral infection or exposure to IFN in a gene-specific manner. Lastly, our results demonstrated that EtOH attenuates the antiviral function of the ADH-ALDH pathway, which suggests the possibility that EtOH-retinol metabolic competition is one of the molecular mechanisms for the synergism between HCV and alcohol abuse in liver disease progression. *Conclusions:* RA plays a critical role in the regulation of intracellular antiviral innate immunity in hepatocytes. (HEPATOLOGY 2016;63:1783-1795)

SEE EDITORIAL ON PAGE 1759

Over 200 million people worldwide are chronically infected with hepatitis C virus (HCV).[1] In the United States, at least 3.5 million people suffer from chronic HCV infection with recent significant increase observed among intravenous (IV) drug users.[2,3] Of particular note, half of the HCV-infected population in the United States has been reported to be heavy drinkers.[4] This group of patients exhibits pronounced HCV replication and refractoriness to antiviral therapy, which results in a 30- and 48-fold increase in developing decompensated cirrhosis and hepatocellular carcinoma, respectively.[5] This synergism between chronic HCV infection and alcohol abuse is well recognized; however, the underlying molecular pathophysiology has not been well understood.

Abbreviations: ADH, alcohol dehydrogenase; APAP, acetaminophen; ATRA, all trans retinoic acid; ALD, alcoholic liver disease; bp, base pairs; CYP2E1, cytochrome P450-2E1; DMEM, Dulbecco's modified Eagle's medium; DR5, direct repeat 5; EtOH, ethanol; GC, gas chromatography; GFP, green fluorescent protein; HCV, hepatitis C virus; HCV-SGR, HCV subgenomic replicon; HPLC-EC, high-performance liquid chromatography with electrochemical detection; HSCs, hepatic stellate cells; IFN, interferon; ISGs, interferon-stimulated genes; IV, intravenous; Jak, Janus kinase; MOI, multiplicity of infection; NAD+, nicotinamide adenine dinucleotide; NAPQI, N-acetyl-p-benzoquinone imine; PAMPs, pathogen-associated molecular patterns; PHHs, primary human hepatocytes; RA, retinoic acid; RAL, retinaldehyde; RAR, retinoic acid receptor; RARE, retinoic acid response element; ROL, retinol; RT-PCR, reverse-transcription polymerase chain reaction; RE, retinyl ester; RIG-I, retinoic acid-inducible gene I; RXR, retinoid X receptor; SeV, Sendai virus; STAT, signal transducer and activator of transcription; UTR, untranslated region.

Received December 16, 2014; accepted December 1, 2015.

Additional Supporting Information may be found at onlinelibrary.wiley.com/doi/10.1002/hep.28380/suppinfo.

This work was supported by funds from AASLD/ALF Liver Scholar Award, Baxter Foundation Award, SCRC for ALPD & Cirrhosis Pilot Project Grant (5P50AA011999) and USC RCLD pilot grant (5P30DK048522), NIAAA (R21AA022751), NIDDK (RO1DK101773), ACS IRG (to T.S.), and NIGMS (P20GM103408; to J.R.C.).

View this article online at wileyonlinelibrary.com.

DOI 10.1002/hep.28380

Potential conflicts of interest: Dr. James is part owner of Acetaminophen Toxicity Diagnostics, LLC. ATD is a recipient of grant R42DK079387 from NIDDK to develop a clinical laboratory test for acetaminophen protein adducts.

Hepatocytes play a central role in ethanol (EtOH) metabolism through alcohol dehydrogenase (ADH) and, to a lesser extent, through cytochrome P450-2E1 (CYP2E1) oxidation to acetaldehyde.[6] Acetaldehyde is subsequently metabolized to acetate by aldehyde dehydrogenase (ALDH).[6] The relevance of metabolic by-product(s) of EtOH and/or cellular response in the pathogenesis of HCV has not been well understood, primarily because of the lack of appropriate research tools. Here, we established Huh7 cell-line based systems that express individual enzymes required in EtOH metabolism. Of great interest, our results demonstrate that the ADH-ALDH pathway serves as a potent antiviral element; whereas, CYP2E1 is a proviral host factor. We also found that the antiviral phenotype of the ADH-ALDH pathway is significantly attenuated in the presence of EtOH.

ADH also plays a critical role in the conversion of retinol (ROL) to retinaldehyde (RAL), followed by the oxidation of RAL to retinoic acid (RA) by ALDH.[7] For ADH1, which is abundantly expressed in hepatocytes, ROL is the far preferred substrate as compared to EtOH. However, the ROL concentration in serum is much lower than the ADH1 Km for ROL. In contrast, the blood EtOH concentration of heavy drinkers often approaches or surpasses the ADH1 Km for EtOH, thus providing a situation in which biogenesis of RA is impaired.[7,8] This led us to hypothesize that EtOH-ROL metabolic competition might be an underlying mechanism for the synergism between HCV and alcoholism.

Numerous studies indicate that RA exhibits antiviral activities against a variety of pathogens.[9-11] The antiviral properties of RA have been mainly explained in the context of professional innate immune cells and adaptive immunity[12]; however, the role in innate immunity in terminally differentiated nonimmune cells such as hepatocytes remains undefined. Interferon (IFN)-stimulated genes (ISGs), constituting over 300 genes, represent the antiviral innate immune effectors that cooperatively restrict the viral life cycle.[13] ISG expression at basal levels determines cellular susceptibility to viral infection.[14] During infection, host cells robustly induce additional ISGs upon pattern recognition receptor sensing of pathogen-associated molecular patterns (PAMPs), such as viral genome.[15] This event also results in the secretion of endogenous type 1 IFN, such as IFN-β. IFN then promotes expression of the grossly redundant ISGs in both infected and neighboring cells by activation of Janus kinase/signal transducer and activator of transcription (Jak-STAT) signaling. The magnitude of the additional ISG induction is a major predictor of clinical outcome.[16] Although a few ISGs have been reported as RA inducible,[15,17,18] the fundamental role of RA in regulation of ISGs has not been determined. Our findings revealed that restoration of the ADH-ALDH pathway in Huh7 cells greatly enhanced ISG expression under both basal and induced conditions in a gene-specific manner, which was associated with successful clearance of the pathogen. Moreover, our study revealed that the EtOH-inducible enzyme, CYP2E1,[19] significantly attenuates RA-mediated gene expression and thus supports viral replication.

In summary, our study demonstrated that impaired biogenesis of RA leads to decreased expression of ISGs in hepatocytes, thereby providing a molecular explanation for the synergism between HCV infection and alcoholic liver disease (ALD).

ARTICLE INFORMATION:

From the [1]Department of Medicine, USC Research Center for Liver Diseases, Division of Gastrointestinal and Liver Diseases, University of Southern California, Los Angeles, CA; [2]Southern California Research Center for ALPD and Cirrhosis, Los Angeles, CA; [3]Bioinformatics Service, Norris Medical Library, University of Southern California, Los Angeles, CA; [4]Veterans Administration Medical Center and Department of Internal Medicine, University of Nebraska Medical Center, Omaha, NE; [5]Department of Cellular and Physiological Sciences, Biomedical Research Center, University of British Columbia, Vancouver, British Columbia, Canada; [6]Department of Pediatrics, University of Arkansas for Medical Sciences, and Arkansas Children's Hospital Research Institute, Little Rock, AR; and [7]Department of Biology, Northwest Nazarene University, Nampa, ID.

ADDRESS CORRESPONDENCE AND REPRINT REQUESTS TO:

Takeshi Saito, M.D., Ph.D.
USC Research Center for Liver Diseases
Division of Gastrointestinal and Liver Diseases
Keck School of Medicine of USC
University of Southern California
2011 Zonal Avenue, HMR 801A
Los Angeles, CA 90033-9141
E-mail: saitotak@usc.edu
Fax: +1-323-442-5425

Materials and Methods

CELLS AND TRANSFECTION

Huh7 cells were maintained as previously described[20] and transfected with TransIT-LT1 (Mirus Bio LLC, Madison, WI) or TransIT-messenger RNA (Mirus Bio LLC). Huh7 stable cell lines expressing hADH1B or hCYP2E1 were established by lentiviral transduction (System Biosciences, Inc., Mountain View, CA). Lentiviral transduction was carried out at multiplicity of infection (MOI) 5 followed by Puromycin selection (2 μg/mL) to established polyclonal (pooled) cell lines. Primary human hepatocytes (PHHs) were obtained from Life Technologies (Carlsbad, CA). Primary mouse hepatocytes of C57BL/6 were obtained from Non-Parenchymal Liver Cell Core at Southern California Research Center for ALPD and Cirrhosis.

VIRUSES

Lentiviral and HCV (JFH1) particle was propagated and tittered as described previously(20).[20] Huh7 subgenomic replicon cells were established through G418 (400 ug/mL) selection upon *in vitro* transcribed subgenome transfection. The HCV pseudoparticle system was propagated as previously described.[21] Sendai virus (SeV) was obtained from Charles River Laboratories (Wilmington, MA), and the infection (10-100 HAU/mL) was conducted in serum-free Dulbecco's modified Eagle's medium (DMEM) for 1 hour at 37°C.

CHEMICAL MEASUREMENT OF EtOH AND ACETAMINOPHEN PROTEIN ADDUCTS

EtOH treatments were carried out at 10, 12.5, and/or 50 mM, which correspond to the physiological blood-alcohol concentration among alcoholics of 0.046%, 0.057%, and 0.229%, respectively.[22] EtOH in the cell-culture medium was measured by gas chromatography (GC) similarly to a previous report.[23] Concentrations of acetaminophen (APAP) protein adducts were measured by high-performance liquid chromatography with electrochemical detection (HPLC-EC), as described previously.[24] Acetaldehyde, acetate, all trans retinoic acid (ATRA), and all trans ROL were obtained from Sigma-Aldrich (St. Louis, MO). EC23 (ATRA analog) was purchased from Tocris. RAR antagonist (4310) was described previously.[25]

STATISTICAL ANALYSIS

P values were obtained using the Student *t* test, and results were considered significant at $P < 0.05$.

Result

RESTORATION OF THE EtOH METABOLIC PATHWAYS IN HUH7 CELLS

The ADH and ALDH families are comprised of 8 and 10 family members, respectively.[6] We first conducted meta-analysis of National Center for Biotechnology Information/Gene Expression Omnibus microarray data to determine the isoforms of ADHs and ALDHs that are predominantly expressed in human hepatocytes. Consistent with previous reports, this analysis demonstrated that hepatocytes express the following isoforms; (1) ADH: ADH1 (A, B, and C), 4, 6, and FE1; and (2) ALDH: ALDH1A1, ALDH2, and ALDH4A1 (Supporting Fig. 1A,B).[26]

Because *in vitro* HCV studies are restricted to use of Huh7 cells, we assessed expression of liver-dominant ADHs and ALDHs in Huh7 cells. The gene and protein expression analysis demonstrated that Huh7 cells lack expression of these ADHs and CYP2E1 (Fig. 1A,B). However, they preserved expression of ALDHs, suggesting that reconstitution of ADHs should restore their EtOH metabolism capability.

Among the enzymes responsible for conversion of EtOH to acetaldehyde in hepatocytes, ADH1 is the most abundant in hepatocytes.[7,26] Thus, ADH1 is known to be the primary ADH involved in liver EtOH metabolism. Next, we tested the enzymatic activity of ADH1B (a delegate of ADH1) on EtOH by determining the reduction rate of nicotinamide adenine dinucleotide (NAD+) conversion to NADH. NAD+ is a coenzyme required for oxidation of EtOH, serving as an electron acceptor; and therefore the conversion rate can be used to indirectly monitor ADH activity.[26] Huh7 cellular lysates upon ADH1B overexpression exhibited potent activity whereas ADH4- and ADH6-expressing cells showed negligible activity (Fig. 1C). Next, we evaluated whether reconstitution of ADH1B or CYP2E1 restores EtOH metabolic function in Huh7 cells. The result showed that overexpression of ADH1B, and CYP2E1, to a lesser extent, restored metabolism to physiological concentrations of EtOH[22] (Fig. 1D).

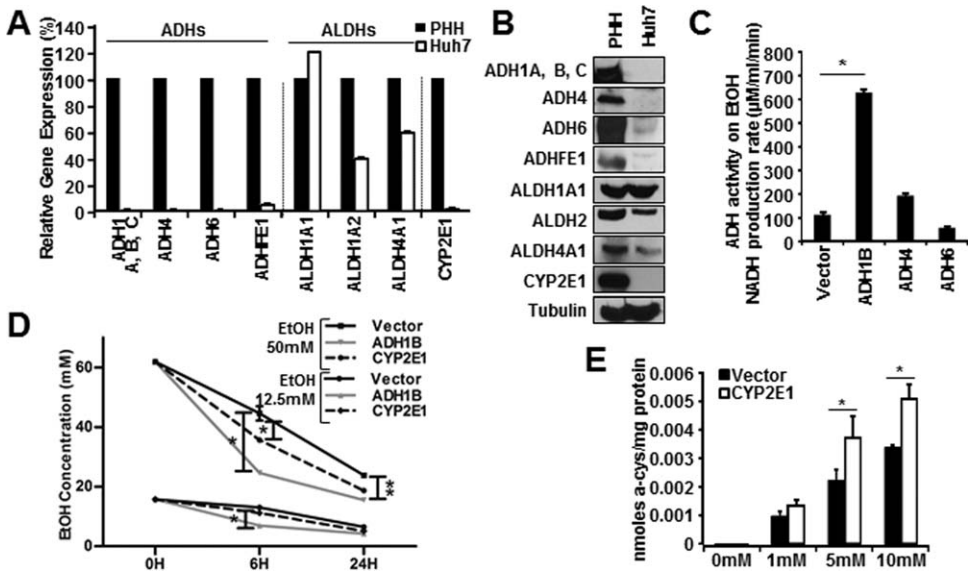

FIG. 1. Restoration of functional EtOH metabolic pathways in Huh7 cells. (A and B). Extracts from either Huh7 or PHHs were subjected to gene expression (A) or immunoblotting (IB) (B) analysis of the indicated enzymes involved in EtOH metabolism. GAPDH was used for normalization to compare relative expression (A). (C) Huh7 cell lysates containing overexpressed ADH isozymes were incubated with NAD (3mM) in the presence or absence of EtOH (10 mM) to assess the NADH conversion rate (μMoles/min/mL). (D) Huh7 cells expressing the indicated vectors were treated with EtOH (12.5 and 50 mM). The culture media were used to measure EtOH concentration by GC. (E) Huh7 cells expressing CYP2E1 were treated with the indicated concentrations of APAP. Concentrations of NAPQI adducts were determined using HPLC-EC. Abbreviation: GAPDH, glyceraldehyde 3-phosphate dehydrogenase.

In addition to CYP1A2, 3A4, and 2D6, CYP2E1 is also known to catabolize xenobiotics such as APAP. Upon metabolism of APAP, CYPs produce the electrophile, N-acetyl-p-benzoquinone imine (NAPQI), which exhibit toxicity through covalent binding to cellular proteins and nucleic acids.[27] Thus, we tested whether CYP2E1 in Huh7 cells produces APAP protein adducts using HPLC-EC. Cell lysates from CYP2E1-expressing cells contained higher NAPQI protein adducts compared to control condition (Fig. 1E). These results assure that Huh7 cells offer an environment for these enzymes to be functional, although these capacities appeared inferior to that of primary hepatocytes likely because of the relative abundance (Supporting Fig. 1C).

THE ADH-ALDH PATHWAY IS A POTENT ANTIVIRAL HOST FACTOR

Restoration of EtOH metabolic capacity in Huh7 cells enabled us to investigate the association between EtOH metabolic pathways and the HCV life cycle. Surprisingly, transient ADH1B overexpression in Huh7 cells harboring HCV subgenomic replicon (HCV-SGR) dramatically suppressed HCV replication (Fig. 2A,B). In contrast, overexpression of CYP2E1 was associated with an enhancement of HCV replication. Moreover, the antiviral effect of ADH1B was reduced in the presence of EtOH (Fig. 2B). Next, we tested whether ADH1B affects the efficiency in establishing viral life cycle by HCV-SGR replicon transduction assay. Transfection of HCV subgenome in Huh7 cells that stably express ADH1B demonstrated a significantly lesser number of HCV-replicating foci formation; however, the difference between control and ADH1B cells diminished upon EtOH treatment (Fig. 2C). These results indicate that the ADH-ALDH pathway serves as an antiviral host factor in the absence of EtOH. Furthermore, our results suggest that either (1) the EtOH metabolic byproducts generated by ADH1B may offer a suitable environment for efficient HCV replication or (2) EtOH prohibits the biogenesis of antiviral molecules produced by the ADH-ALDH pathway. To distinguish between these possibilities, we addressed whether EtOH metabolites increase HCV replication

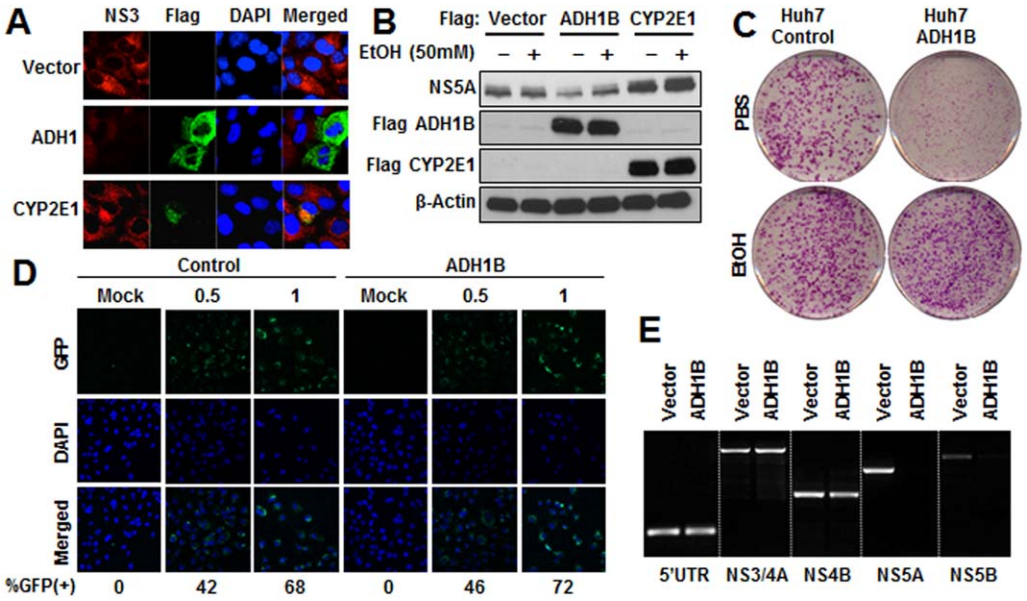

FIG. 2. The ADH-ALDH pathway is a potent antiviral host factor. (A) Huh7 cells harboring HCV-SGR were transduced with the indicted vectors for 48 hours. Extracts were subjected to immune-fluorescent analysis. Red: HCV NS3; green: Flag-ADH1 or CYP2E1; blue: DAPI. (B) The indicated expression vectors were transfected into Huh7 cells containing HCV-SGR for 24 hours followed by EtOH treatment for 48 hours. The extracts were subjected to immunoblotting (IB) analysis. (C) Huh7 cells expressing ADH1B or control vector were transfected with *in vitro* transcribed HCV-SGR genome followed by G418 selection in the presence or absence of EtOH (12.5 mM). Upon completion of G418 selection, the culture dishes were fixed and stained with crystal violet. (D) Huh7 cells stably expressing ADH1B or control vector were challenged with HCV pseudo-particles containing a GFP reporter at the indicated titer. Twenty-four hours postinfection, cells were subjected to fluorescent microscopic analysis. Green: GFP; blue: DAPI. The GFP-positive cells at each condition are shown in %. (E) RT-PCR analysis with primer sets targeting the indicated region of HCV genome. RNA was extracted from Huh7 cells stably expressing ADH1B or control vector 7 days after SGR-RNA transfection. Abbreviations: DAPI, 4′,6-diamidino-2-phenylindole; NS, nonstructural protein; PBS, phosphate-buffered saline.

efficiency. The results showed that neither acetaldehyde nor acetate treatment changed viral replication efficiency (Supporting Fig. 2A,B).

To further understand how the ADH-ALDH pathway suppresses HCV, we assessed the effect of ADH1B expression on each stage of the viral life cycle. First, an HCV pseudo particle containing a green fluorescent protein (GFP) reporter was employed to test the effect of ADH1B expression on viral entry. Under these conditions, ADH1B expression in Huh7 cells was found to have a negligible effect on viral entry (Fig. 2D). Next, we examined the effect of ADH1B expression on genome replication using reverse-transcription polymerase chain reaction (RT-PCR). The abundance of each region of the viral genome decreased with distance from the replication initiation site (5′UTR [untranslated region]) of the viral genome, especially in ADH1B-expressing cells (Fig. 2E). This result may suggest that the ADH-ALDH pathway restricts HCV by promoting premature termination of genome replication. Taken together, these results indicate that the ADH-ALDH pathway restricts HCV at the genome replication/translation stage.

SHARED ANTIVIRAL PROPERTIES OF LIVER-DOMINANT ADH ISOFORMS

We extended our investigations to the other liver-dominant ADHs to determine whether these enzymes also suppress HCV. To accomplish this, we expressed ADH4 and ADH6 in Huh7-SGR cells and assessed their antiviral potency. The result showed that expression of ADH4 and ADH6 in HCV-SGR cells exhibited a comparable degree of viral suppression as to that observed with ADH1B expression (Fig. 3A). Similar results were observed with immunofluorescent microscopic analysis and protein analysis, wherein these ADH isoforms potently inhibited HCV (Fig. 3B,C), indicating that the antiviral activity of ADH is not unique to ADH1B, but is shared among other ADHs.

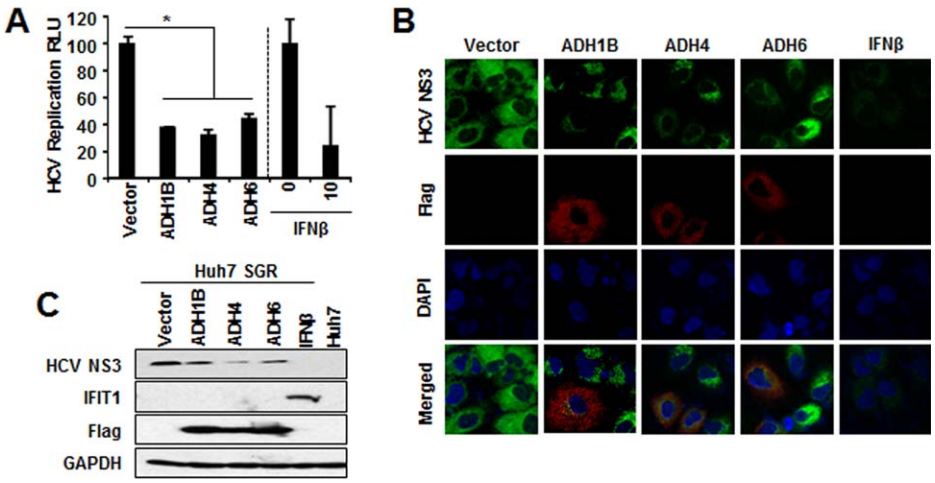

FIG. 3. Shared antiviral properties of liver-dominant ADHs. (A) HCV-SGR cells containing HCV IRES-dependent firefly luciferase reporter were transduced with the indicated expression vectors along with renilla luciferase plasmid for 48 hours. The firefly luciferase values were normalized with renilla luciferase and presented as relative luciferase unit (RLU). $^*P < 0.01$. (B and C) HCV-SGR cells were transfected with the indicated expression vectors for 48 hours followed by immunofluorescent microscopic analysis (green: HCV-NS3; red: Flag; blue: DAPI) (B) or immunoblotting (IB) analysis of the indicated proteins (C). IFNβ 10 IU/mL served as positive control for HCV suppression (A-C). Abbreviations: DAPI, 4′,6-diamidino-2-phenylindole; GAPDH, glyceraldehyde 3-phosphate dehydrogenase; NS, nonstructural protein.

Analysis of ADH enzymatic activity revealed that the different ADHs possess distinctive EtOH metabolic activity (Fig. 1C). These ADHs have also been shown to metabolize ROL,[7,26] leading to the possibility that the ADH-ALDH pathway suppresses HCV through metabolism of ROL. To test this possibility, cell lysates containing these ADH isoforms were treated with ROL in the presence of NAD, and the enzymatic activity was assessed by the rate of NAD+ reduction to NADH. All ADHs tested were found to exhibit comparable activity on ROL (Supporting Fig. 3A). In addition, the antiviral effect of ADH1B but not ADH4 was antagonized by EtOH (Supporting Fig. 3B), likely reflecting the enzymatic activity on EtOH (Fig. 1C) as well as KiEtOH to ROL.[7] These observations collectively suggest that the antiviral activity of ADH may be through the metabolism of ROL to the biogenesis of RA and EtOH impairs the antiviral effect of the ADH-ALDH pathway, depending on their affinity to EtOH.

THE ADH-ALDH PATHWAY REGULATES GENE EXPRESSION THROUGH BIOGENESIS OF RA

To test whether ADH1B expression enables the production of RA from ROL in Huh7 cells, a few well-accepted RA-inducible genes' expression were assessed by quantitative RT-PCR. The result showed that ADH1B-expressing cells robustly induced these genes in response to ROL treatment (Fig. 4A). RA regulates gene expression by binding to the heterodimer nuclear receptor complex that is comprised of retinoic acid receptor/retinoid X receptor (RAR-RXR).[28] The RAR-RXR heterodimer binds preferentially to a retinoic acid response element (RARE), which contains two receptor cognate-binding sequences typically separated by 5 base pairs (bp), direct repeat 5 (DR5). RA binding to the RAR leads to recruitment of coactivators and activation of gene transcription.[28] Therefore, we investigated whether ADH1B expression in Huh7 cells impacts RAR-mediated gene expression using a RARE-containing luciferase reporter. First, a series of RARE luciferase reporters comprising of 1, 3, and 5 bp separated RARE (DR1, DR3, or DR5, respectively) were expressed in Huh7 cells and the response to ATRA treatment was monitored. Addition of ATRA selectively induced significant luciferase activity only in the DR5 RARE reporter (Supporting Fig. 4A). Moreover, the DR5 reporter was found to exhibit increased and reduced activity in response to an RA agonist (EC23) or an RAR antagonist (4310), respectively (Supporting Fig. 4B,C). Given these results, the

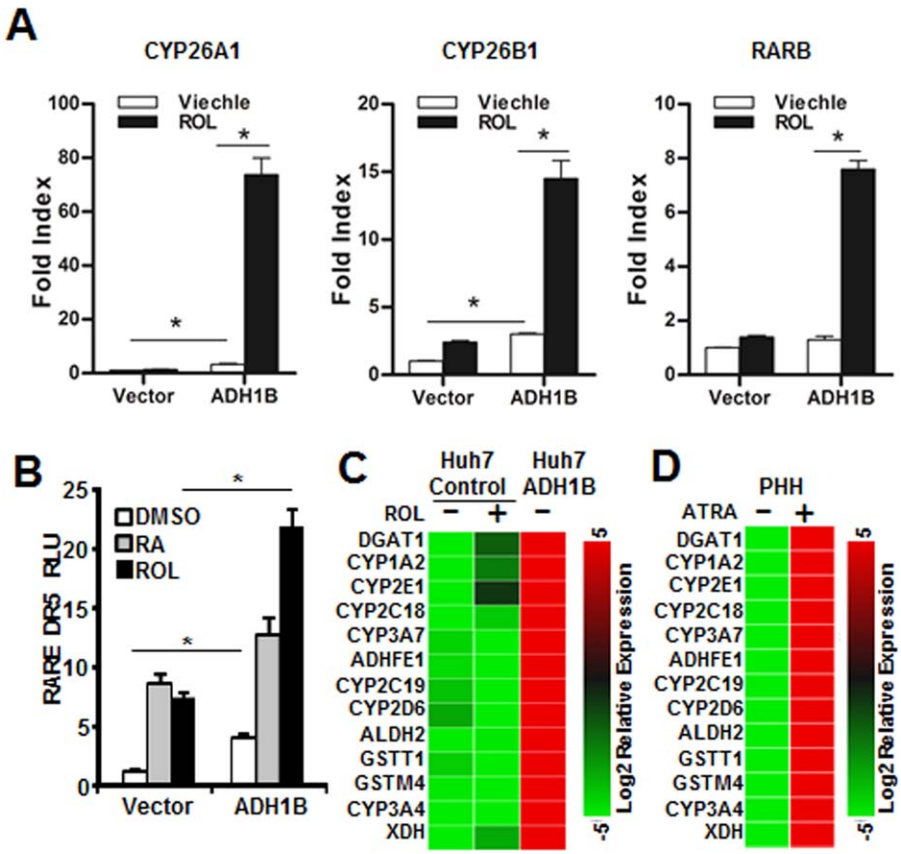

FIG. 4. Reconstitution of the ADH-ALDH pathway restores biogenesis of RA. (A) Huh7 cells expressing ADH1B or control vector were treated with DMSO (vehicle) or ROL (1 μM) for 16 hours. Extracts were subjected to quantitative RT-PCR analysis of the indicated RA-inducible gens. (B) Huh7 cells were cotransfected with the indicated expression vectors, a firefly luciferase reporter regulated by RARE-DR5, and a renilla luciferase vector. Twenty-four hours after transfection, cells were treated with ROL (1 μM), ATRA (0.1 μM), or DMSO for 36 hours followed by dual luciferase assay. (C and D) Extracted RNA from Huh7 cells stably expressing ADH1B or control vector (C) or PHHs (D) were subjected to quantitative RT-PCR array of RA-regulated genes. The heat map represents the relative abundance of the indicated genes. Cells were treated with either ROL (1 μM) (C), ATRA (0.1 μM) (D), or DMSO (control) for 16 hours before RNA extraction. $^*P < 0.01$. Abbreviations: DMSO, dimethyl sulfoxide; RLU, relative luciferase unit.

RARE-DR5 reporter was employed as a surrogate to follow RAR activity. After cotransfection of the RARE-DR5 into Huh7 cells and treatment with ROL, coexpression of ADH1B induced activation of RARE-DR5 (Fig. 4B). In addition, both gene expression analysis and reporter assay results showed that ADH1B expression enhances RA-gene regulation even under the basal condition. We speculate that this is likely because of the metabolism of up to 50 nM of ROL in standard 10% fetal bovine serum DMEM by the ADH1B-ALDH pathway. To further test the influence of the ADH1B-ALDH pathway in gene regulation, a quantitative RT-PCR array comprising RA-regulated genes was employed (Fig. 4C,D). The result demonstrated that ADH1B expression globally up-regulates RA-inducible genes at the basal condition, and the degree of the up-regulation was significantly higher than that of exogenous ROL-treated control Huh7 cells. Next, we compared the gene expression changes observed in Huh7 cells that express ADH1B to that of PHH treated with ATRA. These results showed identical patterns (Fig. 4C,D), thereby indicating that reconstitution of ADH1B in Huh7 cells leads to production of RA from ROL. This notion is also well supported by the fact that the control cells minimally changed the expression of RA-regulated genes even in response to exogenous ROL (Fig. 4A-C).

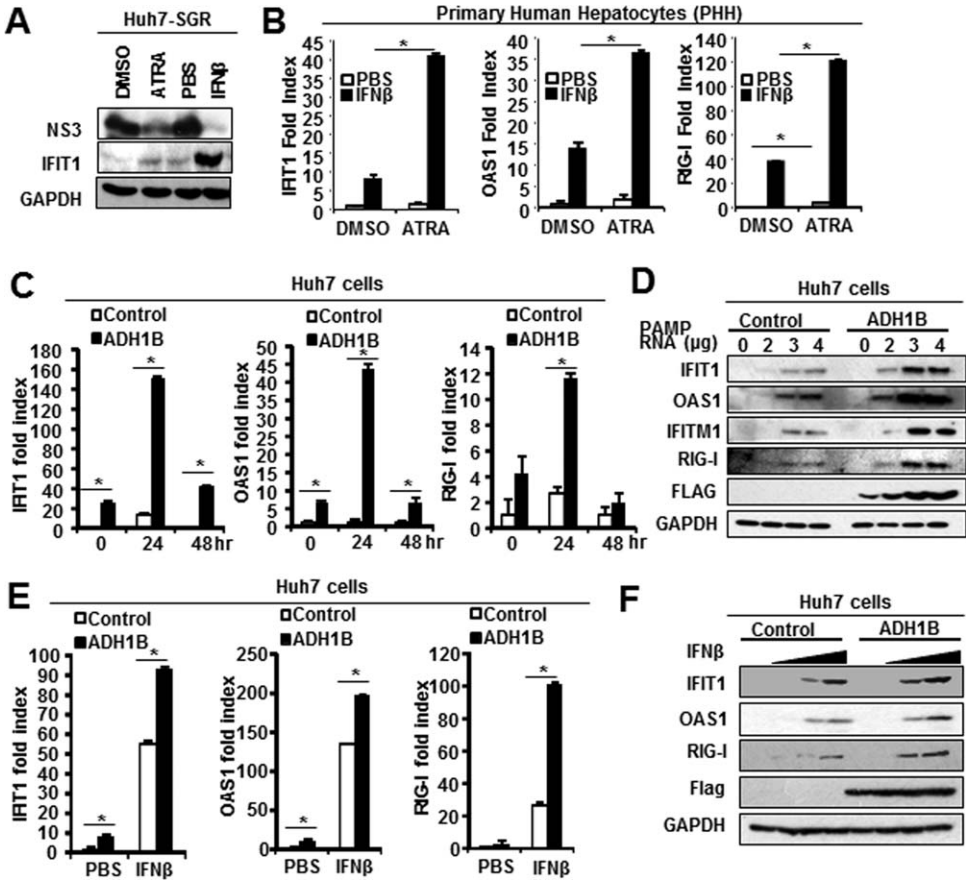

FIG. 5. Potent anti-HCV suppression by RA and its enhancement of ISG expression. (A) Huh7 HCV-SGR cells were treated with ATRA (0.1 μM) or IFNβ (10 IU/mL) for 72 hours. Extracts were subjected to immunoblotting (IB) analysis of the indicated proteins. (B) Quantitative RT-PCR analysis of RNA extracted from PHHs pretreated with ATRA (0.1 μM) or vehicle for 16 hours followed by IFNβ (100 IU/mL) for 8 hours. (C and E) RT-PCR for ISG expression analysis. Huh7 cells stably expressing ADH1B were transfected with HCV-PAMP-RNA (1 $\mu g/5 \times 10^5$cells) for indicated hours (C) or treated with IFNβ (100 IU/mL) for 8 hours (E). $^*P < 0.01$. (D and F) IB analysis of ISG expression. Huh7 cells stably expressing ADH1B were transfected with HCV-PAMP-RNA (0, 2, 3, and 4 $\mu g/5 \times 10^5$cells) for 24 hours (D) or treated with IFNβ (0, 1, 10, and 100 IU/mL) (F). Abbreviations: DMSO, dimethyl sulfoxide; GAPDH, glyceraldehyde 3-phosphate dehydrogenase; NS, nonstructural protein; OAS1, 2′5′-oligoadenylate synthetase 1; PBS, phosphate-buffered saline; RLU, relative luciferase unit.

CRITICAL ROLE OF THE ADH-ALDH PATHWAY FOR THE ISG EXPRESSION

Next, we directly tested whether RA alone was sufficient to suppress HCV. For this purpose, HCV-SGR cells were treated with RA and this led to dramatic inhibition of viral replication (Fig. 5A). RA is known to play an important role in a variety of cellular functions, including cell proliferation, death, and differentiation.[8] To better understand the mechanisms underlying RA suppression of HCV replication, we initially tested whether the ADH-ALDH pathway influences cell growth and/or susceptibility to cell death, which may nonspecifically influence viral replication given that the life cycle heavily relies on the cellular machinery. Expression of ADH1B neither changed cell growth/proliferation nor cell viability (Supporting Fig. 5A,B). These results led us to hypothesize that the ADH-ALDH pathway plays a role in the regulation of antiviral host factors such as ISGs for suppression of HCV.

Clinical studies reported that RA enhances the response to IFN-based antiviral therapy.[11,29] These observations suggest that expression of ISGs could be governed, at least partially, by RA. To further explore

this hypothesis, we conducted a bioinformatics search of ISG (446 genes) promoter and found that 88% of the regulatory region of ISGs contain RARE-DR5 sequence (Supporting Table 1). This observation suggests that up-regulation of ISGs by RA may underlie the ADH-ALDH-mediated suppression of HCV.

To further test this idea, we first investigated whether RA augments the expression of ISGs in terminally differentiated PHHs. These experiments showed that ATRA treatment increased the basal expression level of, at least, a few selected ISGs (Fig. 5B). In addition, the RA treatment significantly enhanced ISG expression in response to type 1 IFN, well supporting aforementioned clinical observations (Fig. 5B). Similarly, the synthetic ATRA analog (EC23) enhanced the IFN-mediated ISG induction in PHHs (Supporting Fig. 5C). These observations with noncancerous primary cells further indicate the critical roles of RA in ISG expression in hepatocytes.

Next, we tested whether the ADH-ALDH pathway enhances expression of ISGs in Huh7 cells. Gene expression analyses showed that ADH1B expression increases ISG expression under basal conditions (Fig. 5C,E). We also tested whether ADH1B expression augments ISG expression in the induced condition with HCV-PAMP-RNA or IFNβ treatment. These are the ligands of two distinct ISG induction pathways: retinoic acid-inducible gene I (RIG-I) or the Jak-STAT pathway,[15] which leads to robust induction of ISGs during infection in infected or neighboring cells, respectively. The result showed that ADH1B expression substantially increased ISG expression in response to these ligands at both the message (Fig. 5C,E) and protein level (Fig. 5D,F). Last, we also found that ADH1B expression has negligible effect on the signaling activation potency by these ligands (Supporting Fig. 5D,E), suggesting that the augmentation of ISG expression by RA is likely at the promoter level.

SELECTIVE UP-REGULATION OF ISGs BY THE ADH-ALDH PATHWAY

Given chromatin remodeling activity of RAR-RXR, we hypothesized that RA regulates ISG expression at the promoter level.[28] Thus, we speculated that the effect of the ADH-ALDH pathway on ISG induction is highly dependent on the accessibility of activated RAR-RXRs to individual gene promoters, rather than indiscriminate global gene up-regulation. Thus, we assessed the pattern of ISG expression in ADH1B-expressing cells using a quantitative RT-PCR array. In agreement with our hypothesis, ADH1B-expressing cells enhanced ISG expression in a gene-specific manner under both basal conditions and during acute HCV (JFH-1) infection (Fig. 6A). Of note, the up-regulated ISGs include well-studied anti-HCV genes, such as IFIT1 and IFITM1. Furthermore, HCV replication efficiency in ADH1B-expressing cells demonstrated an inverse association with the degree of ISG inducibility (Fig. 6B,C). Last, we challenged Huh7 cells expressing ADH1B with SeV, which induces ISGs in a RIG-I signaling-dependent manner similar to HCV.[15] ADH1B expression was found to attenuate viral replication efficiency, which is correlated with degree of ISG induction (Supporting Fig. 6A,B). These observations indicate that the ADH-ALDH pathway restricts viral infection through augmentation of ISG expression at the gene promoter/enhancer level.

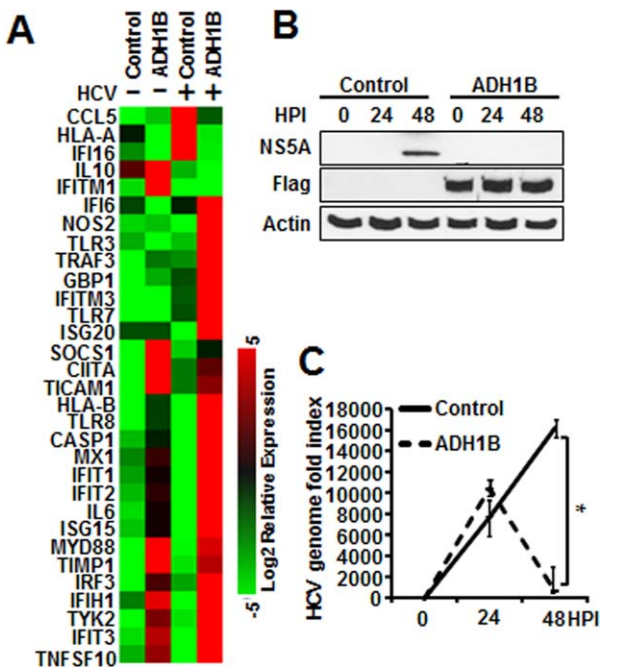

FIG. 6. Selective up-regulation of ISGs governed by the ADH-ALDH pathway protect hepatocytes from HCV infection. (A and C) Huh7 cells stably expressing ADH1B or control vector were infected with HCV (JFH1 MOI: 0.5) for 24 and 48 hours. RNA was extracted 24 hours postinfection (HPI) and used for quantitative RT-PCR array for the detection of a panel of ISGs (A); RNA and protein extracts were subjected to immunoblotting (IB) analysis (B) or quantitative RT-PCR (C) for detection of viral products. *$P < 0.01$. Abbreviation: NS, nonstructural protein.

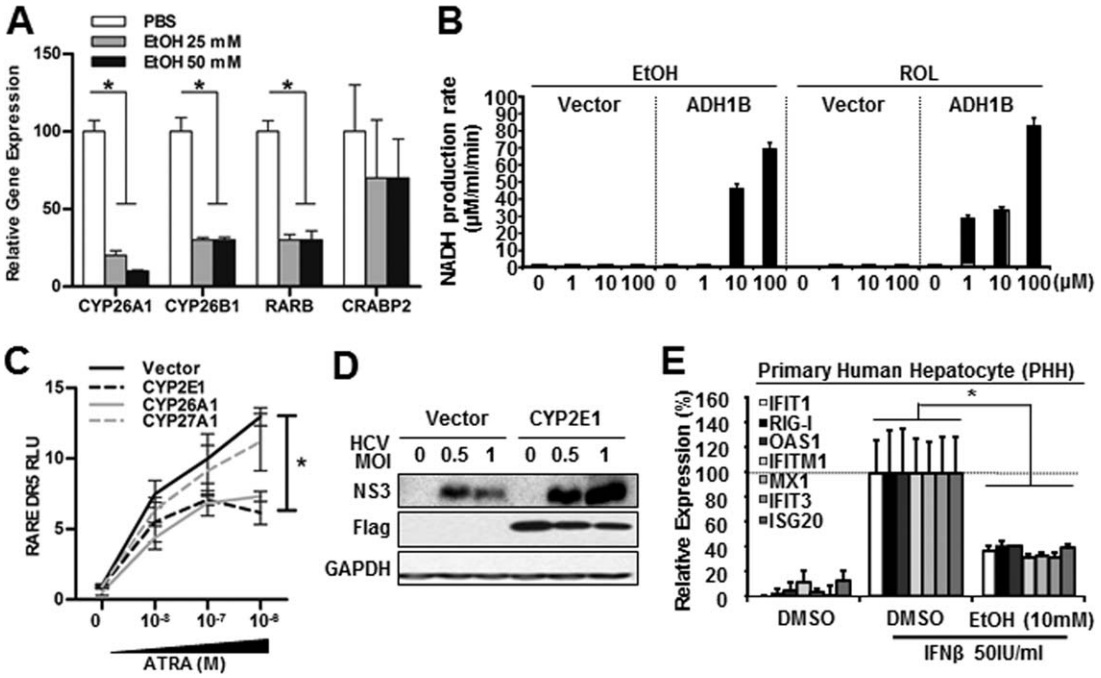

FIG. 7. EtOH deregulation of retinoid homeostasis through two distinct mechanisms. (A) Quantitative RT-PCR analysis of RA-inducible genes. Mouse primary hepatocytes were treated with EtOH for 60 hours. $^*P < 0.01$. (B) Cell lysates expressing ADH1B or control cells were incubated with NAD (3 mM) and indicated ADH substrates. ADH activity was calculated by the rate of NAD+ to NADH conversion (μMoles/min/mL). (C) RARE-DR5 dual luciferase assay. Huh7 cells were cotransfected with the indicated CYP expression vectors, RARE DR5 luciferase, and renilla reporter followed by RA for 36 hours. $^*P < 0.01$. CYP26A1: positive control. CYP27A1, which catabolizes vitamin D, was employed as a negative control. (D) immunoblotting (IB) analysis of HCV protein expression. Huh7 cells were transfected with CYP2E1 or control vector for 24 hours followed by HCV JFH1 infection for 48 hours. (E) Quantitative RT-PCR of the indicated ISG expression. PHHs were treated with EtOH for 24 hours followed by IFNβ (50 IU/mL) for 8 hours. $^*P < 0.01$. Abbreviations: CRABP2, cellular retinoic acid binding protein 2; DMSO, dimethyl sulfoxide; GAPDH, glyceraldehyde 3-phosphate dehydrogenase; NS, nonstructural protein; OAS1, 2′5′-oligoadenylate synthetase 1; PBS, phosphate-buffered saline; RLU, relative luciferase unit.

TWO DISTINCT EtOH METABOLIZING PATHWAYS IMPAIR RA REGULATION OF INTRACELLULAR INNATE IMMUNITY

Our results suggest that the impairment of RA-mediated ISG regulation in hepatocytes serves as, at least in part, an underlying mechanism for pronounced HCV replication among alcoholics. To further test this idea, we assessed whether EtOH attenuates RAR-mediated gene regulation. Indeed, the analysis with the RARE-DR5 reporter system (Supporting Fig. 7A) and quantitative RT-PCR analysis (Fig. 7A) demonstrated that EtOH impaired RA gene regulation in a dose-dependent manner. Accordingly, the cell lysates from ADH1B-expressing cells demonstrated comparable enzymatic activity on both EtOH and ROL, especially at higher concentrations (Fig. 7B). Moreover, the effect of ADH1B in enhancing ISG expression was attenuated in the presence of EtOH (Supporting Fig. 7B). These observations suggest that EtOH-ROL competition attenuates RA-mediated ISG expression.

Recent evidence has shown that CYP2E1 potently catabolize RA to transcription inactive polar metabolites.[30] CYP2E1 is an EtOH-inducible enzyme that plays a role in EtOH metabolism[19] (Supporting Fig. 7C and Fig. 1D). Of note, our results (Fig. 2B) demonstrated that HCV replication was enhanced upon CYP2E1 expression. Thus, we hypothesized that CYP2E1 expression in hepatocytes can be a secondary mechanism that impairs RA regulation of ISG expression. An assay utilizing the RARE-DR5 reporter showed that RA-mediated gene regulation was significantly attenuated in the presence of CYP2E1 both under basal and induced conditions (Fig. 7C and Supporting

Fig. 7D). Interestingly, our observation suggests that CYP2E1 catabolic activity on ATRA is nearly comparable to that of CYP26A1, which is the most critical RA-catabolizing enzyme with the Km/RA ~10 nM.[31] This suggests that CYP2E1 may preferentially catabolize RA, as compared to other substrates such as EtOH or APAP, and may play a role in the impairment of ISG expression. Consistent with our findings with the HCV-SGR system (Fig. 2B), expression of CYP2E1 substantially increased susceptibility to HCV infection (Fig. 7D).

Last, we tested the effect of EtOH in ISG expression with human primary hepatocytes, in which both EtOH-ROL competition on the ADH-ALDH pathway and CYP2E1 induction contribute to depletion of RA. The results showed EtOH treatment dramatically impaired expression of ISGs (Fig. 7E).

Discussion

Alcohol is the most common intoxicating substance in the United States. Alcoholics are known to have a significantly higher risk of acquiring HCV, owing to the high prevalence of IV drug use in this population.[32] The combination of HCV infection and alcohol abuse rapidly progress to end-stage liver diseases[5,33]; however, the molecular mechanism underlying this phenomenon has been unclear.

Our study demonstrated that the ADH-ALDH pathway is a potent antiviral pathway. We also found that the antiviral effect of ADH-ALDH pathway is mediated by the metabolism of ROL to the biogenesis of RA. Moreover, the antiviral property of the ADH-ALDH pathway was diminished in the presence of physiological concentration of EtOH among alcoholics,[34] likely owing to EtOH-ROL metabolic competition.

The majority of dietary retinoid is stored as retinyl ester (RE) mainly in hepatic stellate cells (HSCs).[35] These stored retinoids are distributed as ROL or RE to maintain serum retinoid concentration. The metabolism of uptaken ROL utilizes a two-step oxidative processe, in which medium-chain ADHs or retinol dehydrogenases catabolize ROL to retinaldehyde, followed by the second oxidation facilitated by ALDH to produce RA.[26] In particular to hepatocytes, ADH1 presumably plays a critical role in biogenesis of RA because of its relative abundance.[36,37]

RA governs various aspects of cell biology, especially in the regulation of cell differentiation and proliferation.[8] Thus, it is thought that RA has great influence on cells continuously undergoing proliferation and differentiation, such as professional immune cells. Indeed, RA is known to potentiate adaptive immunity by regulating T-cell proliferation, T helper 1-2 balancing, and cytotoxicity, as well as modulating B-cell proliferation and immunoglobulin production.[12] However, the role of RA in intracellular innate antiviral immunity, in which ISGs play a central role, has not been determined.

The contribution of RA in ISG induction appears not unique only to genes which nomenclature contains "RA inducible."[15,17,18] Indeed, a number of ISGs were noted to be up-regulated in the gene list obtained from transcriptome analysis of ATRA-treated leukemia cells.[38] Our results indicated that the effect of RA in ISG induction is gene specific rather than global up-regulation (Fig. 6A), suggesting that RA unlikely induces ISGs by secretion of IFNs nor confers activation of ISG induction pathways. In fact, we did not observe the phosphorylation of STATs and interferon regulatory factor 3 in ATRA-treated cells (data not shown) or ADH1B expression in Huh7 cells (Supporting Fig. 5D,E). These notions collectively suggest that RA augments ISG expression at the gene promoter level. Our bioinformatics analysis demonstrated that the occurrence of RARE-DR5 in promoters of randomly selected genes was 2.11475 (-5,000 to +500). Based on this number, we categorize ISGs into: (1) high DR5: >= 4 (82 ISGs, average 4.904 DR5 occurrence); (2) medium DR5: >=2 and <4 (204 ISGs, average 2.441 DR5 occurrence); and (3) low DR5: <2 (160 ISGs, average 0.688 DR5 occurrence; Supporting Table 1. These results indicate that RA can influence the expression of up to 88% of ISGs at the promoter level. Moreover, the occurrence of RARE-DR5 is significantly higher in nearly 20% of ISG promoters, further suggesting the role of RA in ISG expression. However, we have also noted that the RARE-DR5 frequency is not well correlated to the degree of ISG expression enhanced by the ADH-ALDH pathway (Fig. 6A; Supporting Table 1). This can be explained either by the cell-type-based differential response to RA or the discrepancy between the bioinformatics algorithms and the actual RAR-RXR occupancy. In fact, a study by others has noted differential RA-gene regulation in a cell-type-specific manner and have shown that genome-wide RAR binding loci do not correspond to expression of RA target genes.[39] The study attributed this discrepancy to the diversity of RAR-RXR binding sequence and/or chromatin topology.

Our study found that the ADH-ALDH pathway restricts HCV life cycle at either protein translation and/or genome replication stage. Because a similar pattern of HCV suppression was observed in IFN-treated HCV-SGR cells (data not shown), it is possible to speculate that the ISGs up-regulated by the ADH-ALDH pathway cooperatively drive this phenomenon. Because these two stages of viral life cycle have great influence on each other, further investigation is required in order to precisely define the mechanism of how RA-regulated ISGs exhibit antiviral activities.

Our results also imply the possibility that catabolism of RA by CYP2E1 may contribute to the impairments of ISGs expression. In addition, others have reported that the oxidative stress triggered by CYP2E1 impairs the IFN-mediated ISG expression through inhibition of STAT1 tyrosine phosphorylation,[40] indicating that CYP2E1 impairs ISG expression through multiple mechanisms. Furthermore, chronic liver diseases such as ALD and HCV infection are known to cause hypovitaminosis A as a result of the myofibroblastic transformation of HSCs.[29,41] This mechanism likely further aggravates the impairment of RA-regulated ISG expression and thus explains the refractoriness to IFN-based antiviral therapy among advanced liver disease patients.

In summary, our study provided novel insights on the pathophysiology behind the synergistic liver disease progression between HCV infection and ALD. The insights obtained from our study are well applied to the high-risk demographics of HCV infection, given that nearly half of infected populations are heavy drinkers.

Acknowledgment: The authors thank T. Tellinghuisen (The Scripps Research Institute) and M. Gale (University of Washington) for reagents and Dr. Jessica Y. Rathbun and EeLyn Ooi for technical assistance.

REFERENCES

1) Gravitz L. Introduction: a smouldering public-health crisis. Nature 2011;474:S2-S4.
2) Edlin BR, Carden MR. Injection drug users: the overlooked core of the hepatitis C epidemic. Clin Infect Dis 2006;42:673-676.
3) Edlin BR, Eckhardt BJ, Shu MA, Holmberg SD, Swan T. Toward a more accurate estimate of the prevalence of hepatitis C in the United States. HEPATOLOGY 2015;62:1353-1363.
4) Russell M, Pauly MP, Moore CD, Chia C, Dorrell J, Cunanan RJ, et al. The impact of lifetime alcohol use on hepatitis C treatment outcomes in privately insured members of an integrated health care plan. HEPATOLOGY 2012;56:1223-1230.
5) Peters MG, Terrault NA. Alcohol use and hepatitis C. HEPATOLOGY 2002;36(5 Suppl 1):S220-S225.
6) Crabb DW, Matsumoto M, Chang D, You M. Overview of the role of alcohol dehydrogenase and aldehyde dehydrogenase and their variants in the genesis of alcohol-related pathology. Proc Nutr Soc 2004;63:49-63.
7) Chase JR, Poolman MG, Fell DA. Contribution of NADH increases to ethanol's inhibition of retinol oxidation by human ADH isoforms. Alcohol Clin Exp Res 2009;33:571-580.
8) Balmer JE, Blomhoff R. Gene expression regulation by retinoic acid. J Lipid Res 2002;43:1773-1808.
9) Villamor E, Koulinska IN, Aboud S, Murrin C, Bosch RJ, Manji KP, Fawzi WW. Effect of vitamin supplements on HIV shedding in breast milk. Am J Clin Nutr 2010;92:881-886.
10) Neuzil KM, Gruber WC, Chytil F, Stahlman MT, Graham BS. Safety and pharmacokinetics of vitamin A therapy for infants with respiratory syncytial virus infections. Antimicrob Agents Chemother 1995;39:1191-1193.
11) Bocher WO, Wallasch C, Hohler T, Galle PR. All-trans retinoic acid for treatment of chronic hepatitis C. Liver Int 2008;28:347-354.
12) Mora JR, Iwata M, von Andrian UH. Vitamin effects on the immune system: vitamins A and D take centre stage. Nat Rev Immunol 2008;8:685-698.
13) Schoggins JW, Rice CM. Interferon-stimulated genes and their antiviral effector functions. Curr Opin Virol 2011;1:519-525.
14) Cho H, Proll SC, Szretter KJ, Katze MG, Gale M, Jr., Diamond MS. Differential innate immune response programs in neuronal subtypes determine susceptibility to infection in the brain by positive-stranded RNA viruses. Nat Med 2013;19:458-464.
15) Saito T, Owen DM, Jiang FG, Marcotrigiano J, Gale M. Innate immunity induced by composition-dependent RIG-I recognition of hepatitis C virus RNA. Nature 2008;454:523-527.
16) Sen GC. Viruses and interferons. Annu Rev Microbiol 2001;55:255-281.
17) Mao M, Yu M, Tong JH, Ye J, Zhu J, Huang QH, et al. RIG-E, a human homolog of the murine Ly-6 family, is induced by retinoic acid during the differentiation of acute promyelocytic leukemia cell. Proc Natl Acad Sci U S A 1996;93:5910-5914.
18) **Yu M, Tong JH**, Mao M, Kan LX, Liu MM, Sun YW, et al. Cloning of a gene (RIG-G) associated with retinoic acid-induced differentiation of acute promyelocytic leukemia cells and representing a new member of a family of interferon-stimulated genes. Proc Natl Acad Sci U S A 1997;94:7406-7411.
19) Takahashi T, Lasker JM, Rosman AS, Lieber CS. Induction of cytochrome P-4502E1 in the human liver by ethanol is caused by a corresponding increase in encoding messenger RNA. HEPATOLOGY 1993;17:236-245.
20) Ooi EL, Chan ST, Cho NE, Wilkins C, Woodward J, Li M, et al. Novel antiviral host factor, TNK1, regulates IFN signaling through serine phosphorylation of STAT1. Proc Natl Acad Sci U S A 2014;111:1909-1914.
21) Bartosch B, Dubuisson J, Cosset FL. Infectious hepatitis C virus pseudo-particles containing functional E1-E2 envelope protein complexes. J Exp Med 2003;197:633-642.
22) Brick J. Standardization of alcohol calculations in research. Alcohol Clin Exp Res 2006;30:1276-1287.
23) Clemens DL, Halgard CM, Miles RR, Sorrell MF, Tuma DJ. Establishment of a recombinant hepatic cell line stably expressing

alcohol dehydrogenase. Arch Biochem Biophys 1995;321:311-318.
24) Muldrew KL, James LP, Coop L, McCullough SS, Hendrickson HP, Hinson JA, Mayeux PR. Determination of acetaminophen-protein adducts in mouse liver and serum and human serum after hepatotoxic doses of acetaminophen using high-performance liquid chromatography with electrochemical detection. Drug Metab Dispos 2002;30:446-451.
25) Dranse HJ, Sampaio AV, Petkovich M, Underhill TM. Genetic deletion of Cyp26b1 negatively impacts limb skeletogenesis by inhibiting chondrogenesis. J Cell Sci 2011;124:2723-2734.
26) Duester G. Families of retinoid dehydrogenases regulating vitamin A function: production of visual pigment and retinoic acid. Eur J Biochem 2000;267:4315-4324.
27) James LP, Capparelli EV, Simpson PM, Letzig L, Roberts D, Hinson JA, et al. Acetaminophen-associated hepatic injury: evaluation of acetaminophen protein adducts in children and adolescents with acetaminophen overdose. Clin Pharmacol Ther 2008;84:684-690.
28) Bastien J, Rochette-Egly C. Nuclear retinoid receptors and the transcription of retinoid-target genes. Gene 2004;328:1-16.
29) Bitetto D, Bortolotti N, Falleti E, Vescovo S, Fabris C, Fattovich G, et al. Vitamin A deficiency is associated with hepatitis C virus chronic infection and with unresponsiveness to interferon-based antiviral therapy. HEPATOLOGY 2013;57:925-933.
30) Liu C, Russell RM, Seitz HK, Wang XD. Ethanol enhances retinoic acid metabolism into polar metabolites in rat liver via induction of cytochrome P4502E1. Gastroenterology 2001;120:179-189.
31) Lutz JD, Dixit V, Yeung CK, Dickmann LJ, Zelter A, Thatcher JE, et al. Expression and functional characterization of cytochrome P450 26A1, a retinoic acid hydroxylase. Biochem Pharmacol 2009;77:258-268.
32) Falk D, Yi HY, Hiller-Sturmhöfel S. An epidemiologic analysis of co-occurring alcohol and drug use and disorders: findings from the National Epidemiologic Survey of Alcohol and Related Conditions (NESARC). Alcohol Res Health 2008;31:100-110.
33) Bhattacharya R, Shuhart MC. Hepatitis C and alcohol: interactions, outcomes, and implications. J Clin Gastroenterol 2003;36:242-252.
34) Vonghia L, Leggio L, Ferrulli A, Bertini M, Gasbarrini G, Addolorato G. Acute alcohol intoxication. Eur J Intern Med 2008;19:561-567.
35) Friedman SL. Hepatic stellate cells: protean, multifunctional, and enigmatic cells of the liver. Physiol Rev 2008;88:125-172.
36) Deltour L, Foglio MH, Duester G. Metabolic deficiencies in alcohol dehydrogenase Adh1, Adh3, and Adh4 null mutant mice. Overlapping roles of Adh1 and Adh4 in ethanol clearance and metabolism of retinol to retinoic acid. J Biol Chem 1999;274:16796-16801.
37) Duester G. Involvement of alcohol dehydrogenase, short-chain dehydrogenase/reductase, aldehyde dehydrogenase, and cytochrome P450 in the control of retinoid signaling by activation of retinoic acid synthesis. Biochemistry 1996;35:12221-12227.
38) **Zheng PZ, Wang KK, Zhang QY, Huang QH**, Du YZ, Zhang QH, et al. Systems analysis of transcriptome and proteome in retinoic acid/arsenic trioxide-induced cell differentiation/apoptosis of promyelocytic leukemia. Proc Natl Acad Sci U S A 2005;102:7653-7658.
39) Delacroix L, Moutier E, Altobelli G, Legras S, Poch O, Choukrallah MA, et al. Cell-specific interaction of retinoic acid receptors with target genes in mouse embryonic fibroblasts and embryonic stem cells. Mol Cell Biol 2010;30:231-244.
40) McCartney EM, Semendric L, Helbig KJ, Hinze S, Jones B, Weinman SA, Beard MR. Alcohol metabolism increases the replication of hepatitis C virus and attenuates the antiviral action of interferon. J Infect Dis 2008;198:1766-1775.
41) Blaner WS, O'Byrne SM, Wongsiriroj N, Kluwe J, D'Ambrosio DM, Jiang H, et al. Hepatic stellate cell lipid droplets: a specialized lipid droplet for retinoid storage. Biochim Biophys Acta 2009;1791:467-473.

Author names in bold designate shared co-first authorship.

Supporting Information

Additional Supporting Information may be found at onlinelibrary.wiley.com/doi/10.1002/hep.28380/suppinfo.

Supplemental Figure 1

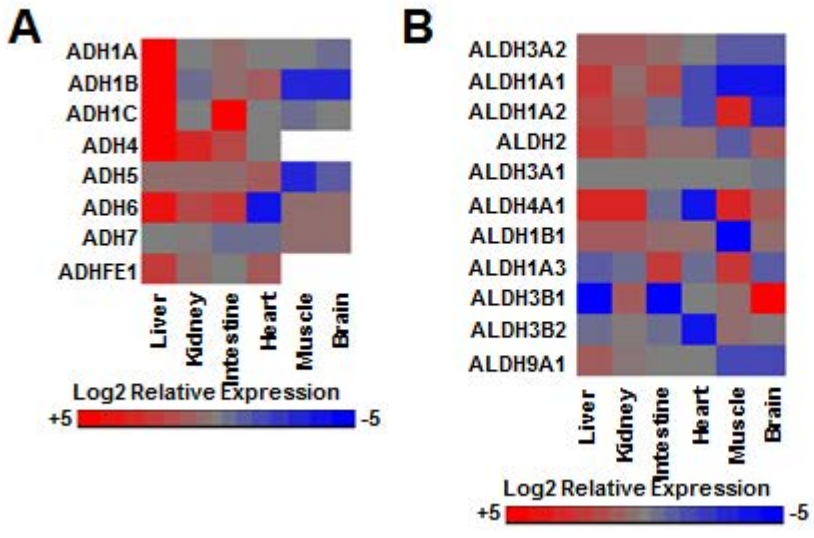

Supplemental Figure 2

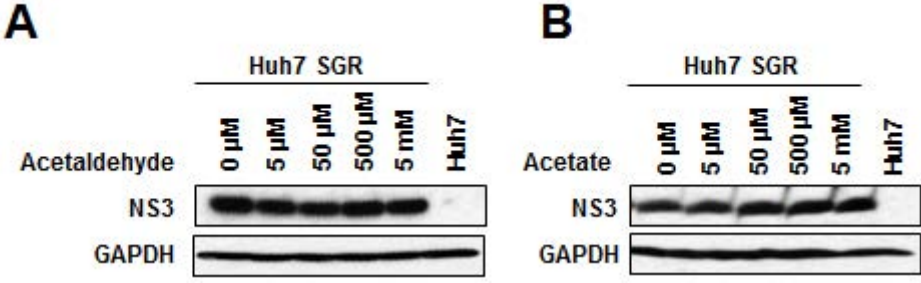

Supplemental Figure 3

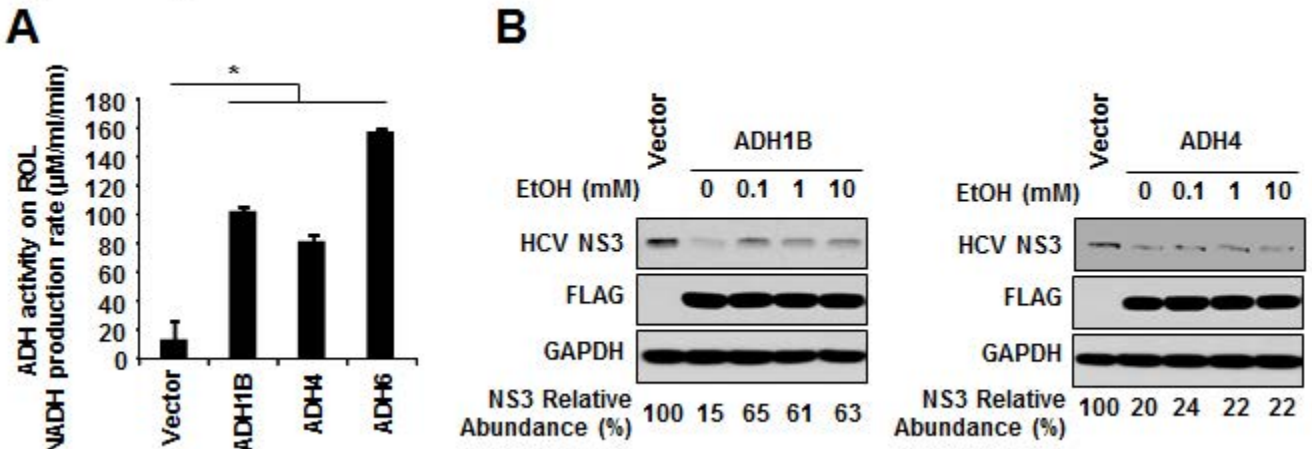

Supplemental Figure 4

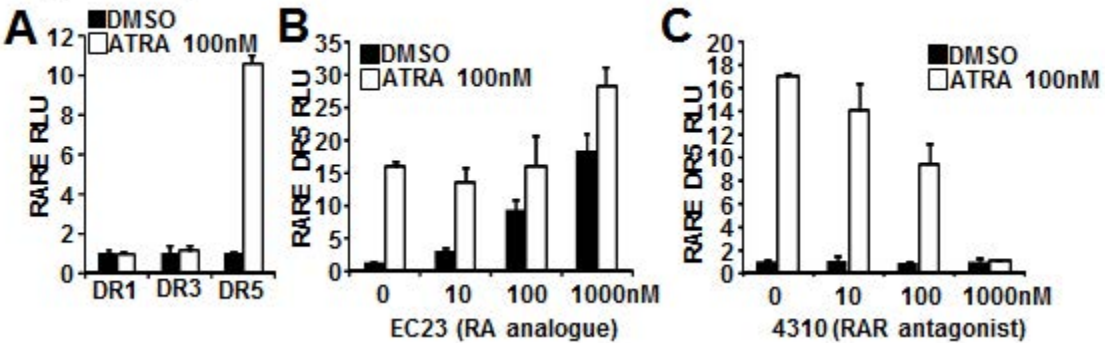

Supplemental Figure 5

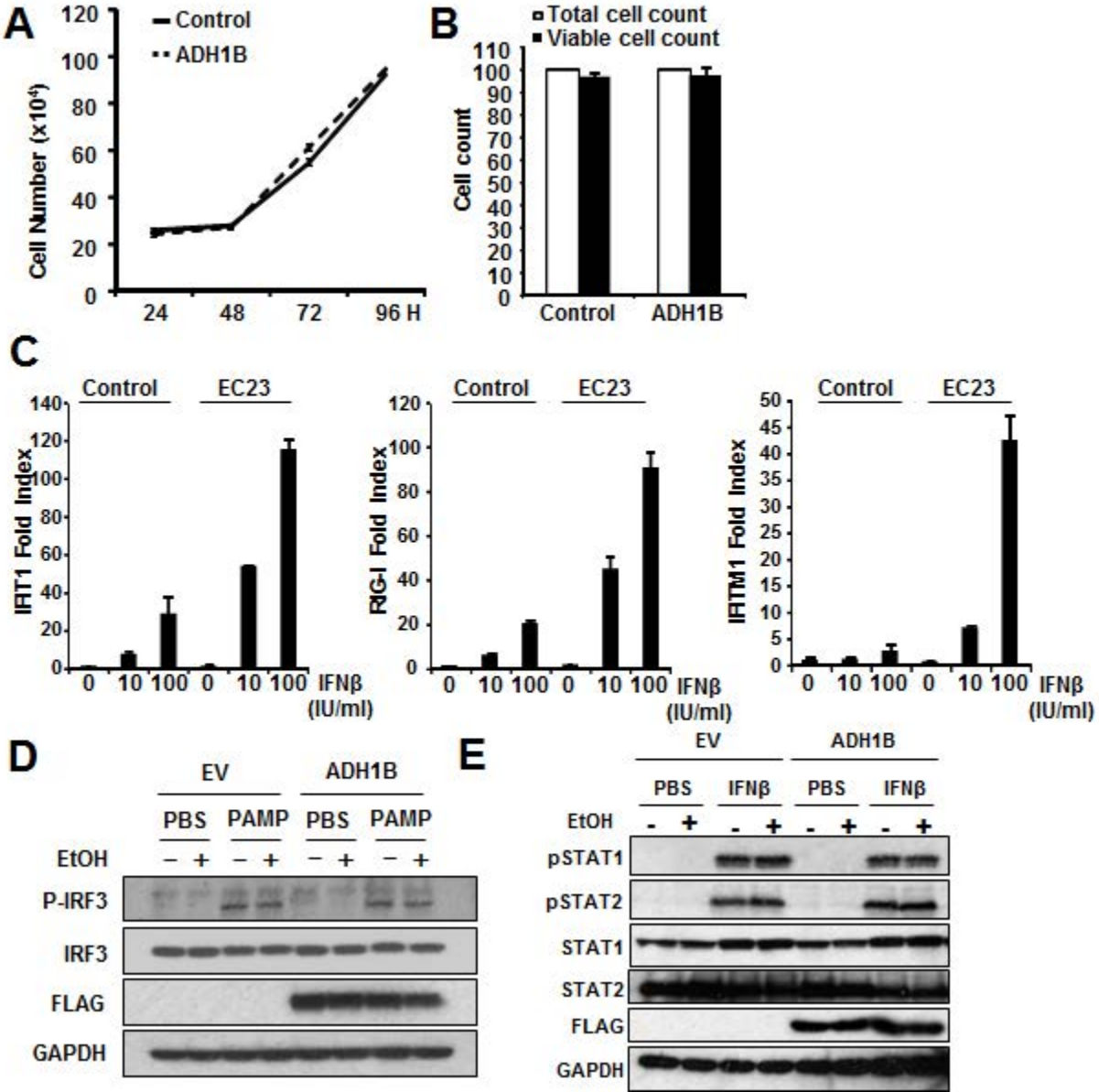

Supplemental Figure 6

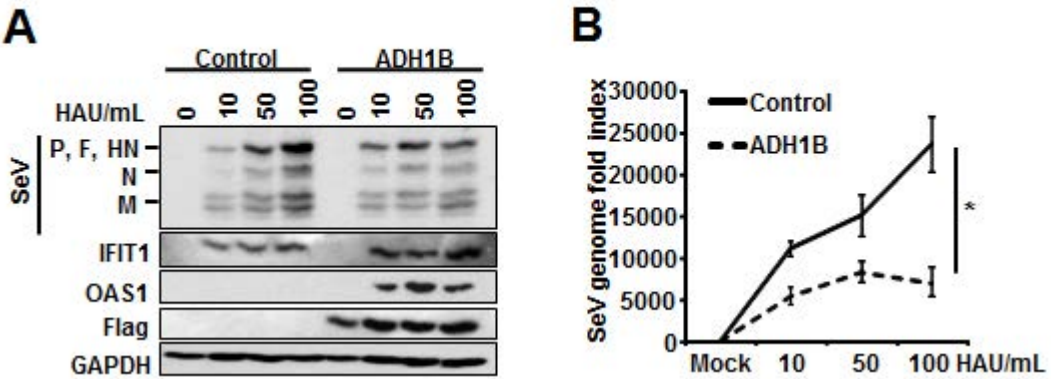

Supplemental Figure 7

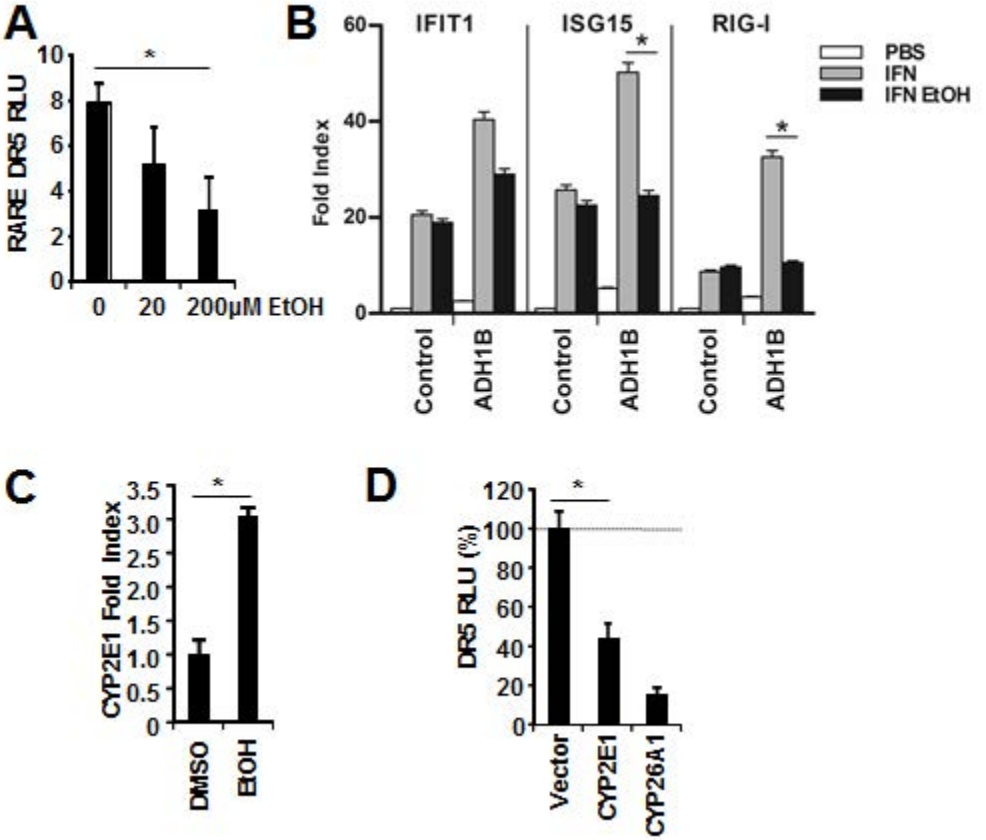

Supplemental Information

Antibodies: The following antibodies were used: mouse anti-HCV NS5A;9E10 (a gift from C. Rice, Rockefeller University), rabbit anti-HCV NS3 (Abcam), rabbit anti-ADH1B (Abcam), rabbit anti-ADH4 (Aviva System Biology), ADH6 (Aviva System Biology), rabbit anti-ADHFE1 (GeneTex), rabbit anti-CYP2E1 (Abcam), rabbit anti-ALDH1A1 (Abcam), rabbit anti-ALDH2 (Abcam), rabbit anti-ALDH4A1 (GeneTex), mouse anti-GAPDH (GeneTex), Flag M2 (Sigma-Aldrich), IFIT1 (a gift from G. Sen, Cleveland Clinic), mouse anti-OAS1 (Kineta), mouse anti-IFITM1 (ProSci), rabbit anti-MX1 (Aviva System Biology), rabbit anti-RIG-I (Cell Signaling), rabbit anti-pIRF3 (Cell Signaling), mouse anti-IRF3 (Biolegend).

Bioinformatics: Bioinformatics: ISG gene regulatory region analysis: The ExPlain^{TM} v3.1 (www.biobase-international.com/explain) from BIOBASE Corporation(1) was used to scan for potential binding sites of RAR-RXR. A list of 446 ISGs was formed based on the data set included in previous publications(2-4) and uploaded into ExPlain. Match function was used to scan for possible binding sites of RAR-RXR in the [-5000, 500] regions around best-supported TSS for the 446 ISGs using position-based weight matrix V$RXRRAR_01 (M02272) with minimized false negatives (minFN) options. To obtain the background occurrence of RAR-RXR in human genome, 500 human genes were randomly selected and scanned using Match with the same parameters. All 446 ISGs were used as enrichment background to minimize any enrichment biases.

Nucleic Acid, Plasmid and Luciferase reporter assay: In vitro transcription of HCV genome or subgenomes was carried out using MEGAscript T7 transcription kit (Life Technologies). HCV PAMP RNA was generated similarly to previously described(5). Cellular RNA extraction was carried out using the RNAeasy kit (QIAGEN). QPCR was conducted using SYBR green-based one-step RT-qPCR method (Life Technologies). The relative gene expression was normalized to GAPDH values to obtain fold increases. The primer sequences for RT-qPCR and expression vector construction are available upon request. RT-qPCR array for the evaluation of Retinoic Acid target genes or ISG expression was conducted using Retinol Metabolism Panel (BioRad) or Type I IFN response panel (QIAGEN) a two-step RT-QPCR. The obtained delta-CT values were analyzed with RT2 Profiler PCR Array Data Analysis version 3.5 and converted to a heat map after exclusion of redundancy, unrelated genes, or genes not expressed in the cells tested. The relative amplitude effect in log2 scale are listed in Table 2. The transient expression or lentiviral expression constructs were generated in pEF Myc/His Version C (Life Technologies) or pCDH-CMV-MCS-EF1-Puro (System Bioscience). All plasmids used in this study were propagated in DH5α under Ampicillin selection and purified with ZR plasmid miniprep or ZymoPure Plasmid Midiprep kit (Zymo Research). Luciferase based reporter assays were carried out with a RARE sequence driven firefly luciferase reporter construct with Dual Luciferase Assay kit (Promega)(6). The inducibility of RARE luciferase (Firefly) was normalized with the value from co-transfected CMV promoter driven Renilla luciferase to determine Relative Luciferase Unit (RLU).

References for Supplemental Information

1. Kel A, Voss N, Valeev T, Stegmaier P, Kel-Margoulis O, Wingender E. ExPlain: finding upstream drug targets in disease gene regulatory networks. SAR QSAR Environ Res 2008;19:481-494.

2. Schoggins JW, Wilson SJ, Panis M, Murphy MY, Jones CT, Bieniasz P, Rice CM. A diverse range of gene products are effectors of the type I interferon antiviral response. Nature 2011.

3. He XS, Nanda S, Ji X, Calderon-Rodriguez GM, Greenberg HB, Liang TJ. Differential transcriptional responses to interferon-alpha and interferon-gamma in primary human hepatocytes. J Interferon Cytokine Res 2010;30:311-320.

4. Bolen CR, Ding S, Robek MD, Kleinstein SH. Dynamic expression profiling of type I and type III interferon-stimulated hepatocytes reveals a stable hierarchy of gene expression. Hepatology 2014;59:1262-1272.

5. Saito T, Owen DM, Jiang FG, Marcotrigiano J, Gale M. Innate immunity induced by composition-dependent RIG-I recognition of hepatitis C virus RNA. Nature 2008;454:523-527.

6. Weston AD, Chandraratna RA, Torchia J, Underhill TM. Requirement for RAR-mediated gene repression in skeletal progenitor differentiation. J Cell Biol 2002;158:39-51.

Supplemental Figure 1. Identification of liver dominant ADH/ALDH isoforms. A-B. Meta-analysis of ADH and ALDH expression: Nextbio was used to obtain the expression profiles of ADH and ALDH in public datasets. In Nextbio, high-quality public microarray dataset from GEO and other genomic data repositories were selected, normalized and pre-calculated for cross-study comparisons. Relative expression of a gene (fold-change) was calculated as the ratio between its expression in the selected tissue and its median expression across 52 tissue groups that are derived from 1067 arrays. For ADH/ALDH expression analysis, 11 liver (GSE3526, GSE1133, GSE2361, GSE7307), 4 kidney (GSE1133, GSE2361, GSE7307), 3 small intestine (GSE2361, GSE7307), 2 heart (GSE2361, GSE7307), 2 smooth muscle (GSE1133), 2 whole brain (GSE1133) tissue samples were analyzed. Relative expression of multiple microarray probes for the same gene were consolidated using the median ratio. **C.** The relative expression abundance of flag-tagged ADH1B or CYP2E1 in Huh 7 cells were compared to that of freshly isolated primary human hepatocytes (PHH). The Huh7 cells were ectopically expressed with the indicated EtOH metabolizing enzymes for 24 hours. Then cell lysates were subjected to immunoblotting analysis for a relative abundance comparison with the cell lysates of freshly isolated PHH.

Supplemental Figure 2. The effect of EtOH metabolic byproduct on HCV replication. A-B. Huh7 cells stably harboring HCV subgenomic replicon (JFH1 strain) were treated with acetaldehyde (**A**) or acetate (**B**) at indicated concentration for 48 hours. Cell lysates were then subjected to IB analysis for the detection of HCV protein (NS3). Naïve Huh7 lysates were used as a negative control for HCV.

Supplemental Figure 3. Distinct enzymatic activity of liver dominant ADH isoforms for the catabolism of ROL and its susceptibility to EtOH inhibition. A. Cell lysate expressing indicated ADH were incubated with NAD (3mM) in the presence or absence of ROL (100μM) to assess NAD-NADH conversion rate (μMoles/min/ml) via detection of 340/440nm fluorescent. **B.** Huh7 cells harboring HCV SGR was transduced with a control vector, ADH1B (Left Panel), or ADH4 (Right Panel) for 24 hours. Then cells were treated with the indicated concentration of EtOH for 24 hours followed by IB analysis of the indicated protein. The signal intensity of HCV NS3 was quantified with ImageJ software and the value was normalized to the signal from control vector transfected cells that were treated with PBS. The values are shown in %.

Supplemental Figure 4. RA regulation of gene transcription through the activation of RARE DR5. A-C. Huh7 cells were co-transfected with indicated RARE luciferase and renilla luciferase reporter for 24 hours. Cells were then treated with ATRA treatment alone at 100nM (**A**), co-treated with EC23 (**B**), or 4310 (**C**) at the indicated concentration for 36 hours. Cell lysates are then subjected to dual luciferase assay.

Supplemental Figure 5. RA augment both basal and induced expression of ISG in hepatocytes. A-B. Huh7 cells stably expressing ADH1B or control vector are monitored for the rate of cellular proliferation every 24 hours up to 96 hours (**A**) or subjected to trypan blue staining to determine the viable cells (**B**) at 72 hours. **C.** Freshly isolated primay human hepatocytes were treated with vehicle (DMSO) or EC23 for 16 hours followed by IFNβ treatment for 8 hours at indicated dose. The RNA was subjected to

RT-qPCR for the detection of indicated ISG. **D-E.** Huh7 cells were transfected with either ADH1B or control vector for 24 hours. 8 hours after expression vector transfection, cells were treated with EtOH (25mM) for 16 hours followed by HCV–PAMP RNA transfection (2μg/5x10^5cells)(**D**) or IFN-β (100IU/ml)(**E**). 16 hours after RNA transfection(**D**) or 1 hours after IFN-β treatment, cell lysates were subjected to IB analysis of the indicated protein expression analysis.

Supplemental Figure 6. ADH-ALDH decreases cellular susceptibility to RNA virus infection. A-B. Huh7 cells stably expressing ADH1B or control vector were infected with Sendai Virus (SeV) at indicated infection titer for 24 hours. RNA and protein extracted were subjected to IB analysis (**A**) or QPCR (**B**) for the detection of viral product. *p<0.01.

Supplemental Figure 7. Two distinct EtOH metabolizing pathways impair RA-mediated gene regulation. A. Huh7 cells were co-transfected with an ADH1B expression vector, a RARE DR5 luciferase, and renilla luciferase reporter followed by treatment with ROL (1μM) and the indicated concentration of EtOH for 36 hours. Cell lysates were subjected to dual luciferase assay. *p<0.01. **B.** Huh 7 cells stably expressing ADH1B or control vector were treated with PBS or EtOH (25mM) for 40 hours prior to IFNβ (50IU/ml) treatment for 8 hours. Extracted RNA was used for RT-qPCR analysis of indicated ISGs expression. *p<0.01. **C.** Freshly isolated primary human hepatocytes were cultured in the presence of either DMSO (vehicle) or EtOH 10mM for 24 hours followed by QPCR analysis of CYP2E1 expression change. GAPDH

was used for the normalization and the calculation of fold index. *p<0.01. **D.** Huh7 cells were cotransfected with indicated CYP expression vectors, RARE DR5 luciferase, and renilla luciferase reporter for 36 hours. Cell lysates were subjected to dual luciferase assay. CYP26A1 that catabolize RA serves as a positive control. *p<0.01.

Supplemental Table 1

A. ISG containing high frequency of RARE DR5 in gene regulatory region (-5000 to +500)

High	#	High	#
DEFB1	8	ABLIM3	4
DUOXA2	7	APOL6	4
IGFBP2	7	B2M	4
LY6E	7	B4GALT5	4
MX2	7	CMAH	4
ODC1	7	CRP	4
SCO2	7	CXCL9	4
TREX1	7	CYorf15A	4
TYMP	7	DDX60L	4
ANKRD22	6	ELF1	4
ARG2	6	ENPP1	4
C22orf28	6	FUT4	4
CCL2	6	GBA	4
CLEC4D	6	GBP2	4
FAM26F	6	GNB4	4
GK	6	HLA-A	4
LGALS9	6	HLA-DOB	4
RAB4B	6	HLA-G	4
RPL22	6	HMCN2	4
ABTB2	5	IDO1	4
ANGPTL1	5	IL17RB	4
ARNTL	5	ISG20	4
BCL2L14	5	KIAA0040	4
BMI1	5	LGALS3	4
BUB1	5	MT1M	4
C1S	5	P2RY6	4
CCR1	5	PARP14	4
DDO	5	PDK1	4
FAM134B	5	PLA2G2A	4
FAM46C	5	RARB	4
HEG1	5	RARRES3	4
IL1R1	5	RASSF5	4
IL28RA	5	RNF19B	4
IMPA2	5	SAMHD1	4
LAMP3	5	SP110	4
MIA	5	ST3GAL4	4
PIM3	5	TCF7L2	4
PLA1A	5	TMEM140	4
PLEK	5	TRAFD1	4
PUS1	5	WHAMM	4
SERPINE1	5		
UPP2	5		

B. ISG containing average frequency of RARE DR5 in gene regulatory region (-5000 to +500)

Average	#	Average	#	Average	#	Average	#	Average	#
APOBEC3A	3	MAB21L2	3	ADAMDEC1	2	IFI16	2	S100A8	2
AQP9	3	MCL1	3	ALDH1A1	2	IFI35	2	SAMD4A	2
ARHGEF3	3	MKX	3	AMPH	2	IFI44	2	SAMD9L	2
ATF3	3	MOV10	3	ANG	2	IFI6	2	SERPING1	2
BAG1	3	MSR1	3	ANKFY1	2	IFIT3	2	SLC15A3	2
C15orf48	3	MT1G	3	APOL1	2	IFITM1	2	SLC1A1	2
C3AR1	3	MT1H	3	APOL2	2	IFITM3	2	SMAD3	2
C4orf33	3	MT1X	3	BATF2	2	IFNGR1	2	SOCS1	2
CA7	3	MX1	3	BCL3	2	IL15RA	2	SPATS2L	2
CARHSP1	3	MYOF	3	BLVRA	2	IL6ST	2	SPSB1	2
CCL4	3	NAPA	3	BTN3A3	2	ISG15	2	SPTLC2	2
CD38	3	NMI	3	C10orf10	2	KLHL17	2	SRGN	2
CD53	3	NUP50	3	C1orf38	2	LAP3	2	STAT2	2
CDKN1A	3	OAS2	3	C4orf32	2	LIPA	2	STEAP4	2
CLEC2B	3	OPTN	3	C5orf27	2	LRG1	2	TLR2	2
CLEC4E	3	OTUD4	3	CAPN8	2	MAFB	2	TMEM192	2
CSF2RB	3	PARP12	3	CCDC92	2	MAP3K5	2	TMEM50A	2
CSRNP1	3	PMAIP1	3	CCL19	2	MARCKS	2	TMEM51	2
CTSO	3	PNRC1	3	CD163	2	MCOLN2	2	TMEM86A	2
CYTH1	3	PSMB10	3	CD40	2	MEG3	2	TNFAIP3	2
DCP1A	3	RABGAP1L	3	CD80	2	MICB	2	TNFRSF10A	2
DDX58	3	RASGRP3	3	CEBPD	2	MYC	2	TRIM14	2
DNAL4	3	RBCK1	3	CES1	2	MYD88	2	TRIM25	2
DTX3L	3	RBP2	3	CHUK	2	NEURL3	2	TRIM46	2
DUSP5	3	RNF34	3	CPT1A	2	NPAS2	2	TXNIP	2
FCGR1A	3	SAA1	3	CTCFL	2	NRN1	2	VCAM1	2
FNDC3B	3	SLC16A1	3	CTSS	2	NT5C3	2	VEGFC	2
FNDC4	3	SLC25A28	3	CXCL10	2	OAS1	2	WARS	2
G6PC	3	SNN	3	DUOXA1	2	OAS3	2	WNT10B	2
GABBR1	3	SSBP3	3	EIF2AK2	2	PHF11	2	XAF1	2
GAK	3	STARD5	3	ETV6	2	PI4K2B	2	ZNF263	2
GCA	3	STAT1	3	FAM70A	2	PLIN2	2	ZNFX1	2
GLRX	3	SUN2	3	FFAR2	2	PLSCR1	2		
GPX2	3	TAGAP	3	FTSJD1	2	PPM1K	2		
GZMB	3	TBX3	3	GBP1	2	PRIC285	2		
HLA-DPA1	3	THBD	3	GBP4	2	PSMB8	2		
IFI30	3	THOC4	3	GEM	2	PSMB9	2		
IFI44L	3	TLR3	3	GJA4	2	RNASE4	2		
IFIT1	3	TMEM49	3	GTPBP1	2				
IFIT5	3	TNFSF10	3	HERC6	2				
IRF1	3	UBD	3	HESX1	2				
JUNB	3	UBE2L6	3	HLA-DRB1	2				
LMO2	3	UNC93B1	3	HLA-F	2				
LOC285194	3	VAMP5	3	HPSE	2				
		XRN1	3						
		ZBP1	3						

C. ISG containing low frequency of RARE DR5 in gene regulatory region (-5000 to +500)

Low	#	Low	#	Low	#	Low	#
ADAR	1	IFIH1	1	TAP1	1	JAK2	0
AGPAT9	1	IFIT2	1	TAP2	1	LGMN	0
AHNAK2	1	IFITM2	1	TDRD7	1	MAFF	0
AIM2	1	IL15	1	TIMP1	1	MXD1	0
AKT3	1	IL1RN	1	TLK2	1	NCOA3	0
APOBEC3B	1	IRF2	1	TNFSF13B	1	NDC80	0
ATP10D	1	IRF7	1	TRIM22	1	NFIL3	0
BAZ1A	1	ITIH4	1	TRIM31	1	PADI2	0
BLZF1	1	LRRIQ3	1	TRIM38	1	PHF15	0
CASP1	1	MAP2K5	1	TRIM5	1	PTMA	0
CASP7	1	MAP3K14	1	UBE2D4	1	RGS1	0
CCDC75	1	MASTL	1	ULK4	1	RSAD2	0
CCL5	1	MAX	1	USP18	1	SELL	0
CCL8	1	MB21D1	1	ZCCHC2	1	STAP1	0
CD274	1	MS4A4A	1	ZNF385B	1	TNFAIP6	0
CD74	1	MS4A6A	1	ACSL1	0	TP53	0
CD9	1	MT1F	1	ADM	0	TRIM21	0
CDC25B	1	MTHFD2L	1	ARL5B	0		
CDK17	1	NAMPT	1	BST2	0		
CMPK2	1	NLRC5	1	C5orf39	0		
COMMD3	1	NOD2	1	C9orf91	0		
CSDA	1	OASL	1	CCDC109B	0		
CXCL11	1	OGFR	1	CCNA1	0		
CYP1B1	1	PDGFRL	1	CCND3	0		
DUSP6	1	PFKFB3	1	CCRL1	0		
DYNLT1	1	PLAUR	1	CD69	0		
EHD4	1	PLEKHA4	1	CFB	0		
EPSTI1	1	PML	1	CHMP5	0		
ETV7	1	PMM2	1	CREB3L3	0		
EXT1	1	PNPT1	1	CRY1	0		
FAM125B	1	PRAME	1	CX3CL1	0		
FAM46A	1	PRKD2	1	DDIT4	0		
FAM72B	1	PXK	1	DDX3X	0		
FBXO6	1	RAB8B	1	DHX58	0		
FST	1	RASSF4	1	EIF3L	0		
FTSJD2	1	RIPK2	1	EPAS1	0		
FZD5	1	RNF114	1	ERLIN1	0		
GALNT2	1	RNF213	1	FAM111A	0		
GBP5	1	RTP4	1	FKBP5	0		
GCH1	1	SCARB2	1	FLJ39639	0		
GLB1	1	SDS	1	GBP3	0		
GMPR	1	SECTM1	1	GCNT1	0		
GTPBP2	1	SERPINB9	1	HES4	0		
HIST2H2AA	1	SIRPA	1	HK2	0		
HLA-C	1	SLC22A23	1	HSH2D	0		
HLA-DQB1	1	SLC25A30	1	IFI27	0		
HLA-E	1	SLFN5	1	IL18BP	0		
		SOCS2	1	IRF8	0		

Supplemental Table 2

A. Relative gene expression fold index for Figure 4C (Log 2)

	Huh7 Control		Huh7 ADH1B
Gene Symbol	DMSO	ROL (10^{-6}M)	DMSO
DGAT1	1.000	1.838	3.471
CYP1A2	1.000	2.239	32.832
CYP2E1	1.000	2.575	5.065
CYP2C18	1.000	5.177	140.220
CYP3A7	1.000	2.612	24.024
ADHFE1	1.000	0.259	3.794
CYP2C19	1.000	0.858	22.446
CYP2D6	1.000	0.763	26.970
ALDH2	1.000	0.685	3.401
GSTT1	1.000	0.089	3.323
GSTM4	1.000	0.214	2.213
CYP3A4	1.000	7.614	22.499
XDH	1.000	25.570	508.804

B. Relative gene expression fold index for Figure 4D (Log 2)

	PHH	
Gene Symbol	DMSO	RA
DGAT1	1.000	3.178
CYP1A2	1.000	36.480
CYP2E1	1.000	5.134
CYP2C18	1.000	3.645
CYP3A7	1.000	4.195
ADHFE1	1.000	5.126
CYP2C19	1.000	8.189
CYP2D6	1.000	3.493
ALDH2	1.000	2.232
GSTT1	1.000	4.402
GSTM4	1.000	25.859
CYP3A4	1.000	9.345
XDH	1.000	5.261

C. Relative gene expression fold index for Figure 6A (Log 2)

Gene Symbol	Mock Control Cell	Mock ADH1B Cell	HCV Control Cell	HCV ADH1B Cell
CCL5	1.000	2.563	13.618	5.134
HLA-A	1.000	0.367	3.779	0.442
IFI16	1.000	0.152	3.779	0.304
IL10	1.000	1.255	0.613	0.497
IFITM1	1.000	9.769	0.282	0.256
IFI6	1.000	0.784	1.040	1.366
NOS2	1.000	1.109	0.769	3.439
TLR3	1.000	0.034	0.796	5.808
TRAF3	1.000	1.157	1.129	2.577
GBP1	1.000	1.399	1.838	3.366
IFITM3	1.000	0.975	1.745	3.335
TLR7	1.000	-1.247	9.948	27.024
ISG20	1.000	1.006	0.500	1.923
SOCS1	1.000	2.583	1.173	1.704
CIITA	1.000	11.778	3.929	8.294
TICAM1	1.000	3.823	1.758	3.149
HLA-B	1.000	2.563	-1.006	5.134
TLR8	1.000	2.563	0.994	5.134
CASP1	1.000	2.619	0.260	5.608
MX1	1.000	1.848	0.427	2.765
IFIT1	1.000	1.633	0.636	2.497
IFIT3	1.000	1.883	0.917	2.058
IL6	1.000	2.463	0.747	3.921
ISG15	1.000	2.094	0.675	3.317
MYD88	1.000	2.924	1.035	2.765
TIMP1	1.000	2.472	1.087	2.248
IRF3	1.000	2.506	1.434	3.368
IFIH1	1.000	1.648	-1.330	1.702
TYK2	1.000	2.480	1.122	3.017
IFIT3	1.000	1.883	0.917	2.058
TNFSF10	1.000	2.061	0.729	2.428